Corona Onset, Electric field and Ion Current density of a Tri-Electrode System for Electrostatic Separation Processes

Mohamed M. Abouelsaad, Mohamed A. Abouelatta, Abd-Elhadi R. Salama
Faculty of Engineering at Shoubra, Benha University
108 Shoubra st., Cairo, Egypt.
Email: eng_gendya@yahoo.com

***Abstract*- The paper presents a detailed experimental and numerical analysis of the corona characteristics of a proposed "Tri- electrode system"; consisting of an ionizing wire, an adjustable auxiliary wire and a non-ionizing cylinder, for electrostatic separation applications. The three electrodes have the same voltage and placed parallel above a grounded plate. A computational scheme coupling the method of characteristics and the charge simulation method is developed to solve the corona governing equations and to compute spatial distributions of the electric field and current density of the system. An experimental setup is constructed to model the electrodes arrangement. Dependence of the distributions of the electric field and current density on the system's geometrical characteristics is established and assessed both numerically and experimentally. The configuration offers a more controlled and efficient charging process and separation when compared to earlier separators' designs. The computed results compared favorably well with experiments.**

I. INTRODUCTION

Corona discharge, utilizing different types of electrodes, is commonly employed in many electrostatic applications such as electrostatic separation of granular mixtures [1-3]. Several ionizing electrodes' shapes and types; including needles, wires or blades, were proposed, presented and researched in literature in order to characterize their separation performance and to compute their corona onset voltage V_o, electric field strength E, as well as the generated ionic current density J [4–14].

Recently, a popular configuration usually referred to as ‘‘wire-type dual electrode’’ has been developed and extensively researched [9-13]. The term designates a device consisting of an ionizing wire attached to a cylindrical non-ionizing metallic electrode, of the same voltage, which besides its role as a mechanical support has a significant influence on the onset and development of the corona discharge, Fig. 1 (with the wire W_2 removed). The geometrical parameters of the dual wire-cylinder electrode as well as the applied voltage are known to, largely, influence the separator’s operation [4, 5]. However, due to the very limited space of the separator, little control is usually possible over these geometrical parameters (h_1, h_2 and D) and consequently over the performance of the separator.

The paper presents a new electrode design termed here a "Tri-electrode" or alternatively "a switchable dual electrode", Fig.1, which would allow a wider and smoother control of the corona onset voltage. An adjustable auxiliary small wire W_2 is inserted in the gap between the ionizing wire W_1, parallel to it and having the same voltage, and the cylinder. Unlike the dual electrode configuration in which the electric field strength of the ionizing wire is influenced by the presence of only the cylindrical electrode, this field is highly modulated, for the Tri-electrode system, by the presence of both the auxiliary wire W_2 and the cylindrical support. The proposed design takes advantage of the electric field modulation which would result at the surface of the ionizing wire in order to provide flexible control over the corona onset voltage and consequently the overall corona performance of the separator. It must be noted that throughout this work the, auxiliary wire is considered to be in a non ionizing state and that the only source of ions is the wire W_1.

The corona problem can be readily solved using various techniques such as the finite element, the boundary element method and the method of characteristics and the charge simulation method [15-19]. The present paper employs the coupled technique of the method of characteristics, MOC, and the charge simulation method, CSM, (MOC/CSM) to solve the corona governing equations of the proposed configuration. For the electrostatic case (space charge free), a genetic algorithms–optimized charge simulation method is developed for electric field computations [20].

The paper aims to quantify the performance of the proposed Tri- electrode configuration with regard to its corona characteristics including the onset voltage, the electric field and current density spatial distributions. The study presents the corona physical model adopted for the present case; taking into account a realistic non-uniform charge density distribution at the ionizing wire as a result of the field modulation occurring at its surface. The role of the adjustable auxiliary wire in modulating the surface field of the ionizing wire and switching on/off of the discharge is demonstrated. The results are discussed to assess the influence of the geometrical characteristics of the proposed electrode configuration and to evaluate its merits which would lead to more efficient and better controlled charging process and separation.

II. PHYSICAL MODEL& CORONA GOVERNING EQUATIONS

PHYSICAL MODEL

The corona discharge, for any shape or type of ionizing electrode, is usually characterized by the presence of two

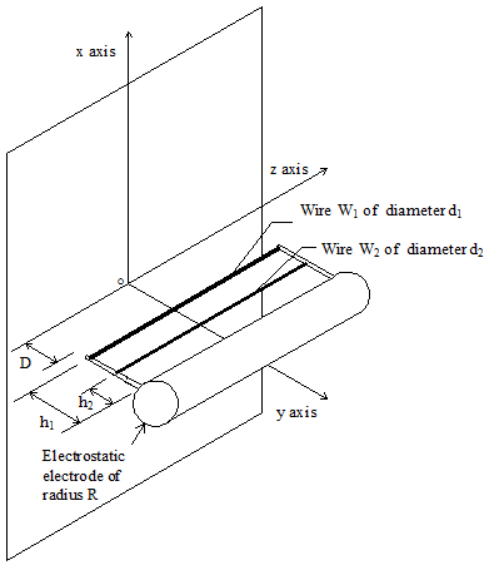

(a)

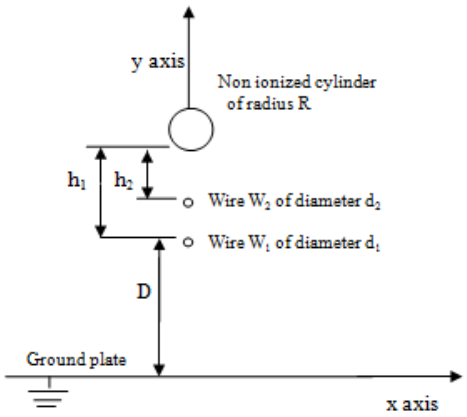

(b)

Fig. 1 (a) Tri-electrode configuration, (b) 2-d representation of the electrode system in (a)

regions: an ionizing thin layer, very close to the active electrode surface, and a drift zone where the ions are driven by the field toward a collecting electrode. To simplify modeling, the ionizing thin layer is considered only as a source of unipolar ions and the study of corona discharge is reduced to the evaluation of the space charge density due to the unipolar ions which move along the field lines. This approach is generally suitable to model the corona electric field, as affected by the ionic space charge [21].

The proposed electrode configuration is shown in Fig. 1. The ionizing wire W_1, the movable auxiliary wire W_2 and the electrostatic cylinder are energized to the same negative potential V. The corona discharge is assumed to take place only at the surface of the wire W_1 (i.e. ionizing electrode). The physical model of the corona discharge adopted for the present study assumes that the unipolar ions leave the surface of the ionizing wire W_1 and move toward the ground plate, in the combined field established by the three electrodes, with a constant mobility k. Both W_2 and the cylindrical electrode are assumed to be in non-ionizing state.

GOVERNING EQUATIONS & BOUNDARY CONDITIONS

The computation domain is assumed to be two-dimensional; neglecting the edge effects of the electrodes and considering that the corona discharge is constant and uniform along the ionizing wire thus the coupled electric field and space charge distributions would be 2-dimensional. The governing equations describing the electric field E in the presence of the negative ions are as follows:

Poisson equation: $\Delta V = - \rho/\varepsilon_0$ (1)

where ρ is the ionic space charge density and V is the electric potential and,

Electric field: $E = - \nabla V,$ (2)

and Current continuity equation: $\nabla . j = 0,$ (3)

where $J = \rho k E$ is the corona current density and k is the ion mobility in m^2/Vs.

For Poisson equation, the boundary conditions are of Dirichlet type for all electrodes (W_1, W_2 and the non-ionizing electrode) with potential V. For the continuity equation (3), the boundary condition consists of imposing a charge density value at all emitting points on the wire surface $\rho_0(\Omega)$. The method that permits to establish the value of ρ_0 (Ω) at each emitting point is based on the Kaptzov's assumption and Peek's relation [22]:

$$E_P = 31\ \delta\ (1+ 0.308/r^{1/2}) \quad (4)$$

where E_P is the corona onset field in kV/cm , δ is the air density and r is the radius of the ionizing wire in cm. Therefore, the boundary condition for the current continuity equation (3) is replaced by Kaptzov's condition that the electric field E at any point Ω on the surface of the ionizing electrode equals the Peek's field and remains constant when the voltage is increased beyond the corona onset level, i.e. $E(\Omega) = E_P$.

The boundary condition of the continuity equation i.e. $\rho_0(\Omega)$ must be adjusted in order to reflect the field modulation at the wire's surface. The condition that the electric field $E(\Omega)$ equals E_P will be assigned, for any point Ω on the wire surface, to simulate the dependence of the value of the charge density on of the position of the point Ω. Any point on the wire will be considered to emit charges only if the local field strength takes a value higher than that given by Peek's relation E_P.

III. COMPUTATIONS OF THE SPACE CHARGE- FREE ELECTRIC FIELD

The calculation of the space-charge-free electric field of the proposed electrode arrangement is the first step in the solution of the ionized field problem governed by equations (1-3). The computation of spatial electric field distribution in the presence of the ionic space-charge consists of the superposition of two

field sources: the potential difference between the electrodes and the electric field created by the ionic space-charge.

The charge simulation method (CSM) is used to calculate the symmetrical 2-D field with the above boundary conditions[23]. Twenty line charges are placed concentric and adjacent to the energized electrodes' inner surfaces with a similar number of boundary points, assigned a potential V, selected along these surfaces. According to the CSM , a matrix equation (5) is set up and solved to determine the magnitude of the simulation charges Q:

$$[P]\,[Q] = [V]\,, \quad (5)$$

$$[F_X][Q] = [E_X] \quad (6)$$

$$[F_Y][Q] = [E_Y] \quad (7)$$

where [P] is the potential coefficient matrix, [Q] is the column vector of unknown charges; [V] is the column vector of known potentials at the contour points. $[F_X]$ and $[F_Y]$ are the electric field intensity coefficients between the simulation charges and the electric field intensity components at the point where the electric field intensity is required in a Cartesian coordinate system. $[E_X]$ and $[E_Y]$ are the components of the electric field intensity at the same point. Given a particular configuration, the coefficients [P] will be determined by the location of the charges and the contour points.

The optimized CSM is a combination of the CSM and genetic algorithms developed to enhance the computational efficiency[20]. A suitable objective function is devised and the simulation charges' number, locations, and their initial estimate values are furnished to the GA/CSM program. Through the evolving generations, the objective function is minimized to obtain the optimal solution. The objective function is:

$$FF = \sum_{j=1}^{Nh} \left[V - v_j\right]^2 \quad (8)$$

where V is the electrode voltage of the ionizing wire, the auxiliary$\sum_{i=1}^{n} P_{ji} Q_i$ wire and the non ionizing cylinder, and Vj= (j=1, 2, … N_h) is the potential obtained by the CSM at the check point j, and N_h is the total number of check points. The developed algorithm is used to solve eq. (5) so that the space charge-free electric field at any space point can be determined.

Maps of equipotential contours are shown in Figs. 2 a &b for two positions of the auxiliary wire, h_2, of 10mm and 16mm. It is seen that the field at the ionizing wire surface becomes highly non uniform due to the presence of the auxiliary wire. This effect increases as the auxiliary wire moves closer to the ionizing wire, i.e. h_2 moves from 10mm to 16mm.

For the given geometry, the GA- CSP can be used to compute the voltage V corresponding to the electric field strength E at the surface of the wire W_1. If V_0 is the corona onset voltage determined experimentally for the same geometry, then the corresponding electric field on the corona wire at onset can be determined as $E_c = E\ (V_0/V)$ [24]

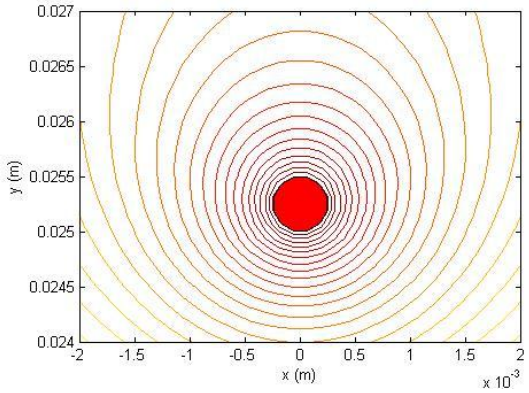

(a)

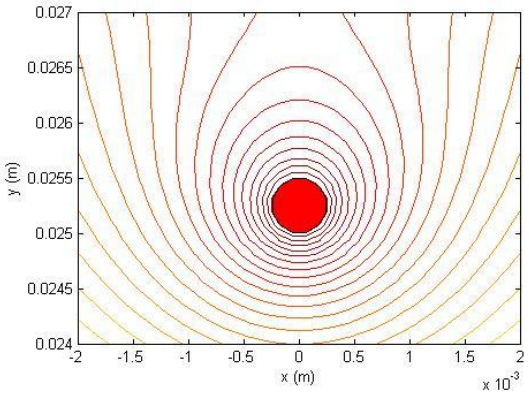

(b)

Fig. 2 Maps of equi-potential contours for the Tri- electrode arrangement ($d_1 = d_2$ =0.5mm, D = 25 mm, h_1=20mm).
(a) h_2=10 mm, (b) h_2=16 mm)

IV. EXPERIMENTAL PROCEDURES

The experimental set-up is shown in Figs. 3a& 3b. The basic configuration consists of two tungsten wires of the same diameter (between 0.3-1.0mm each), both strung parallel to and above a rectangular copper plane- electrode of dimensions 300 mm x 100 mm. The gap clearance D is 25mm. The distance h_1 is varied between 15-25mm and h_2, measured from the cylinder, between 5 and 21mm. For current density measurements, a current probe (a copper strip 100 mm x 10 mm), electrically insulated from the rest of the ground electrode and connected to a micro-ammeter, is used. The electrodes were energized from a negative DC a high-voltage supply (Hipotronics model 800pl- 10mA, 0-80kV).

The measured corona onset voltages are presented in Fig. 4a and 5a for different wire diameters and h_1 values. For each arrangement, the GA-CSP provides the computed electric field strength at the wire surface upon corona onset. Comparison of these results with those computed using Peek's formula is shown in Fig. 4b and 5b.

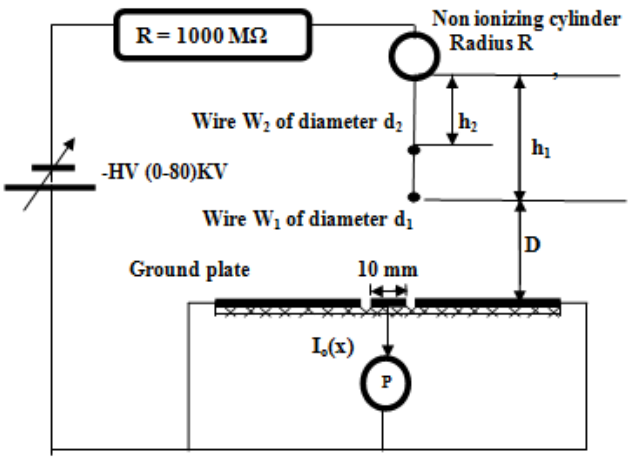

(a)

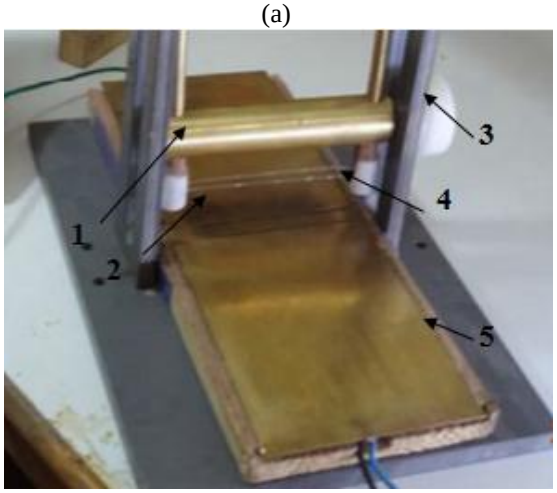

(b)

Fig.3 Experimental setup a) schematic b) geometry of the Tri-electrode system: 1- Non ionizing cylinder, 2- Ionizing wire, 3- Insulating support, 4- Auxiliary wire W_2, 5- Ground plate

Inspection of these results show that the corona onset voltage decreases with the decrease of the wire diameter. As the auxiliary wire moves upward (h_2 decreases), the corona onset voltage decreases. It is observed that the electric field strength at corona onset, Figs.4b, 5b is lower than the values predicted by Peek formula. These results are in agreement with the findings of [24] where it was reported that a correction factor should be applied to Peek's formula for such small wire diameters and multi electrode arrangement. The presence of the auxiliary wire modifies the distribution of the electric field close to the ionizing wire as shown earlier in Fig. 2. As the cylindrical electrode moves closer to the ionizing wire (h_1 =15mm), the corona onset voltage increases and the corresponding electric field decreases as compared to the case of h_1=25mm. The distance between the two wires (h_1-h_2) was kept constant in this case.

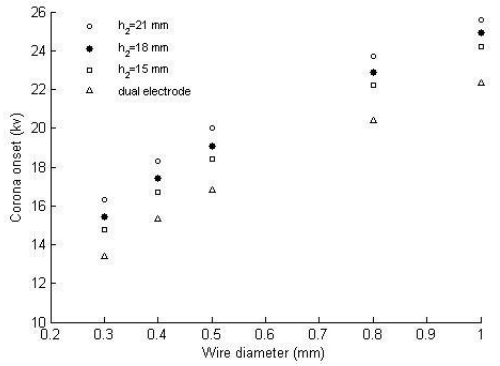

(a)

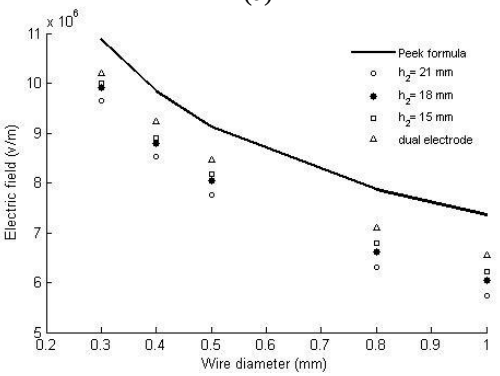

(b)

Fig. 4 Corona onset for different wire diameters, h_1=25mm, (a) Experimental (b) Computed electric field strength at onset

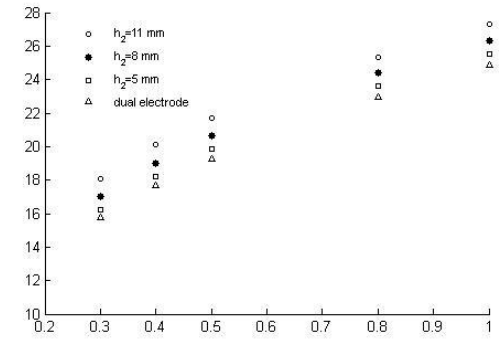

(a)

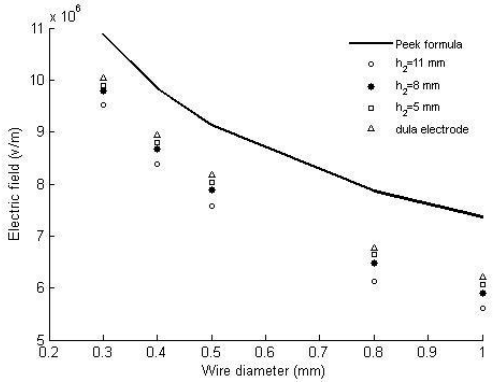

(b)

Fig. 5 Corona onset for different wire diameters, h_1=15mm, (a) Experimental, (b) Computed electric field strength at onset

V. ELECTRIC FIELD MODULATION OF THE TRI- ELECTRODE CONFIGURATION

Earlier studies of the electric field and ion current density, for the dual electrode system, showed that the geometrical characteristics play a very important role for the separator's operation to ensure an efficient particle charging process [11, 24, 25]. In fact, as the large nonionizing cylinder gets closer to the wire, the corona onset voltage of the wire increases, resulting in lower charge emission and vice versa [11, 24, 25]. So, it is possible to obtain higher or lower current without changing the gap D or the applied voltage, for each mixture, to obtain suitable ionic current distribution and maximum particle charging. However, the use of relatively large wire- cylinder clearances, of the dual electrode system, is rather limited in view of the overall small size of the separator. The Tri-electrode configuration overcomes these limitations and provides a more flexible control of the separator's operation as will be demonstrated in the following sections.

Influence of the Auxiliary Electrode Position on Electric Field Modulation

In order to establish the field modulation of the proposed geometry, the GA-CSP program is utilized to compute the electric field strengths E_1 at surface of the wire W_1. The effectiveness of the presence of the auxiliary wire on modulating the electric field around the ionizing wire surface is demonstrated in Fig. 6a. The maximum variation of the surface field is 19.66% for h_2 = 10mm, 23.13% for h_2 = 13 mm and 30.24% for h_2=16mm where D=25mm and h_1=20mm. It is clear that as the auxiliary wire W_2 gets closer to the wire W_1, the surface field on W_1 decreases and becomes more non uniform. The field at the top of the wire surface is more affected than that at the bottom, Fig. 6b, and the corona onset voltage will vary accordingly. This means that by properly positioning the auxiliary electrode, both the corona onset voltage and the level of ionization can be smoothly varied and controlled. In fact, the wire W_1 can be switched to be in an ionizing or non-ionizing state, with all other parameters being the same, by simply positioning the wire W_2 either closer or farther away from W_1. The proposed electrode configuration may thus be termed "switchable dual electrode".

Influence of the Auxiliary Electrode Position on V_0

In view of the above results, Fig. 7 shows the extension of the corona circumference zone, where the field strength at the wire surface is higher than E_p , for different positions of the auxiliary wire W_2. For the given wire radius, the emitting region of the wire depends not only on the applied voltage but also on the location of the auxiliary wire h_2 ; with all other parameters being the same. While the ionizing wire begins to emit at V_0= 19.26kV (h_2=10mm) and V_0= 20.02kV (h_2=13mm) and V_0=21.01kV (h_2=16mm), only for V_0= 23.97 kV , 26.05kV and 30.12kV, for the respective auxiliary wire positions, the entire wire surface would be emitting. In addition, as the auxiliary gets closer to the ionizing wire, the range within which the level of ionization or corona intensity can be controlled to increase/decrease as shown in Fig.8. It should be noted that, for the dual electrode system, these characteristics will be reduced to only one characteristic with a single- valued onset voltage for the system. This clearly demonstrates the distinct role of the auxiliary wire on controlling the corona performance and operation of the separator. Computations and measurements of the field–charge distributions are presented next.

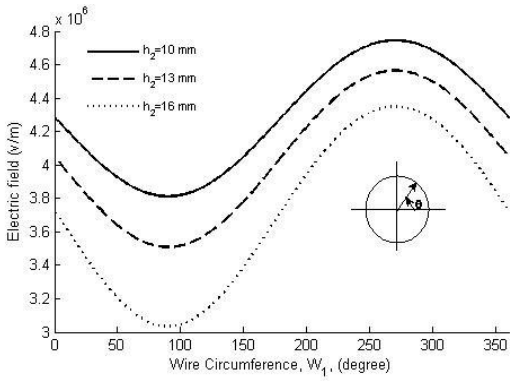

(a)

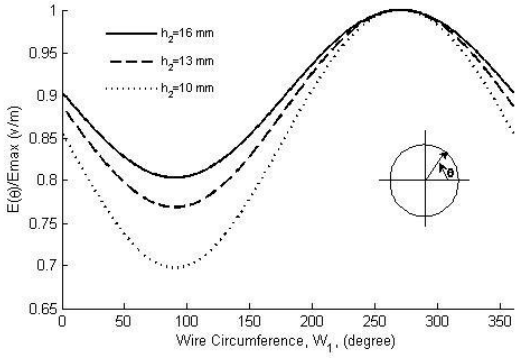

(b)

Fig. 6 Electric field modulation around W_1 for different h_2 (V=10 kV, d_1=d2 =0.5mm, D = 25 mm, h_1=20mm). (a) Variation of electric field, (b) Per unit variation.

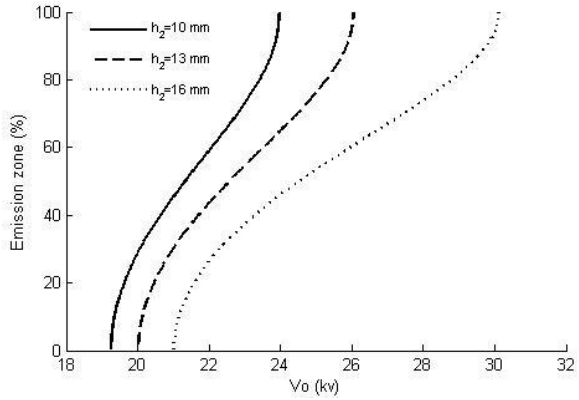

Fig. 7 Influence of the location of the auxiliary wire on the corona discharge zone (d_1=d_2 =0.5mm, D = 25 mm, h_1=20mm)

VI. V-I, ELECTRIC FIELD AND ION CURRENT DENSITY OF THE TRI- ELECTRODE GEOMETRY

A computational algorithm based on the coupled MOC/CSM is developed to solve the corona problem (equations 1-3) for the Tri- electrode configuration. The charge simulation method is used to solve equations (1) and (2) while the method of characteristics (MOC) is employed to solve (3). Both problems are solved iteratively until the solution of the system of equations is reached (the values of V, E, ρ and $\rho_0(\Omega)$ are obtained for all the points of the domain). The method aims to achieve a self-consistent solution of the problem i.e. simultaneously establishing a self consistent electric field and a self consistent space charge distribution. A non-uniform charge distribution on the surface of the ionizing wire is assumed. A two- loop algorithm is developed. Within the inner loop, the spatial distributions of the electric field and space charge density are updated at the end of the loop. The computational process continues with the charge distribution, at any point on the wire surface, being modified in an outer loop until the computed field on the wire surface is equal to Peek's value E_P. The algorithm steps are as follows:

1. Input the data: geometrical dimensions, applied voltage, corona onset field
2. Compute the wire surface charges, space charge- free case, using the GA-CSM. Following these steps, two loops are then developed as follows:
3. Generate a grid of elements made by the intersection of the characteristic lines and equipotential contours.
4. Compute the charge density at the grid points by the method of characteristics. Determine the corresponding space charges within each element.
5. Modify the surface charges to satisfy the Dirichlet boundary conditions at all electrodes.
6. Check for a self consistent electric field; if it is acceptable proceed to the next step. If not, modify the surface and space charges and go back to step 3(inner loop).
7. Compute the average electric field at the ionizing wire. If it is acceptable when compared with Peek's value, then a self-consistent space charge field has been obtained and the solution is complete. If this field deviates from Peek's value, modify the charge density distribution at the wire surface and go back to 3 (outer loop).

VII. RESULTS AND DISCUSSION

A computer program was developed to implement the above procedures for solving eqs.(1-3). The computed and measured current- voltage characteristic of the Tri-electrode geometry is shown in Fig. 8. For a given wire diameter, the discharge current is strongly influenced by the position of the auxiliary wire and increases as the distance h_2 decreases. At the same voltage, higher currents are obtained for smaller wire diameters. For the case $d_1=d_2=0.5$mm and at an applied voltage of 26 kV, the total discharge current increases about 18.5%

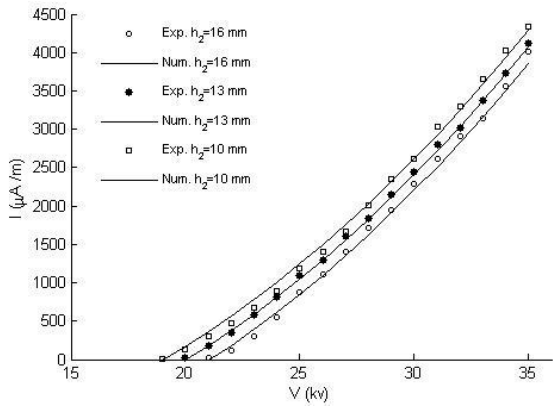

Fig. 8 V-I characteristics for different wire diameters (D = 25 mm, h_1=20mm. $d_1=d_2$ = 0.5mm.

when h_2 changes from 16 mm to 13 mm and by about 15% when h_2 changes from 13 mm to 10 mm. For the case $d_1=d_2$ = 0.8mm, the corresponding values are 54% and 28% respectively. Less variation in the discharge current is observed as the auxiliary wire moves up and away from the ionizing wire as the configuration becomes closer to that of a dual electrode system. Experimental measurements are seen to be in good agreement with the numerical results, Fig. 8.

For different positions of the auxiliary wire, Fig. 9 displays the variation of the computed electric field at the surface of the grounded plate. As h_2 decreases, higher electric field values are obtained with all other parameters being the same. The corresponding current density distributions are shown in Fig. 10. Experimental measurements agree well with the results obtained using the developed numerical algorithm as shown in Fig. 10. It is observed that the spatial extension of theses quantities becomes smaller as the auxiliary wire moves closer (downward) to the ionizing wire. Apparently, the electric field lines (ions trajectories) are contracted and become more confined to a smaller region on the surface of the grounded electrode as h_2 increases. This means that the current density at the surface of the collecting electrode becomes larger or smaller, for a given corona current, depending on whether the auxiliary wire moves closer to the ionizing wire or farther away (upward) from it. Consequently, it is expected that the use of the proposed Tri- electrode system could provide better control over the acceleration of charge accumulation on the particles passing by the collecting electrode in a rather simple, fast and efficient manner. For practical applications, these parameters could be easily adjusted and controlled according to the characteristics of each treated granular mixture for better separator's performance.

VIII. Conclusions

The paper presents experimental and numerical investigations of the proposed Tri- electrode system for electrostatic separation applications. The study demonstrates the system's advantages in furnishing flexible, smooth and fast control of

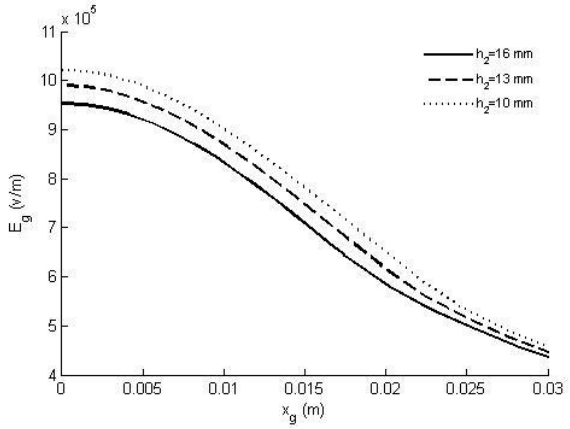

Fig. 9 Electric field distributions at the ground plate for different h_2 (V= 30 kV, D =25 mm, h_1=20mm, d_1=d_2= 0.5mm)

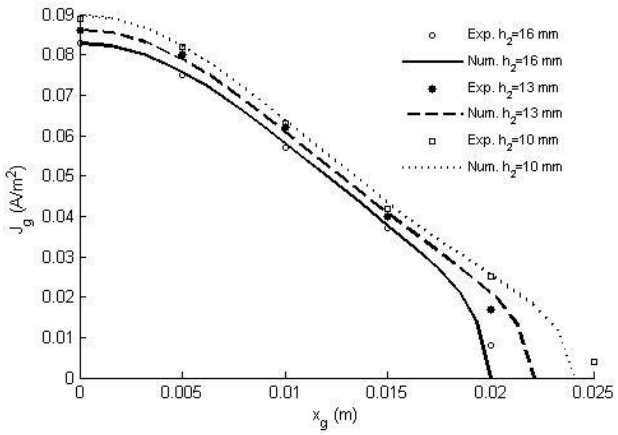

Fig. 10 Current density distributions at the ground plate for different h_2 (V= 30 kV, D =25 mm, h_1=20mm, d_1=d_2= 0.5mm)

the corona onset voltage and level of ionization for a more efficient charging process and separation. The adjustable auxiliary wire provides efficient means for modulating the surface field of the ionizing wire and the ground- level current density profiles and as well the switching on/off of the discharge when necessary. The configuration offers several advantages over earlier separators' designs. Numerical results obtained using the developed computational algorithm compared favorably well with experiments.

References

[1] A.D. Moore (Ed.), Electrostatics and its Applications, Wiley, New York, 1973.

[2] J.S. Chang, A.J. Kelly, J.M. Crowley (Eds.), Handbook of Electrostatic Processes, Dekker, New York, 1995.

[3] Hughes, J.: 'Electrostatic Particle Charging', (Wiley, New York, 1997.)

[4] L.M. Dumitran, O. Blejan, P.V. Notingher, A. Samuila, and L. Dascalescu, Particle charging in combined corona-electrostatic fields, IEEE Trans. Ind. Appl., Vol. 44, pp. 1385-1390, 2008.

[5] M. Kachi, M. Nemamcha, L. Herous, and L. Dascalescu, Neutralization of charged insulating granular materials using AC corona discharge, J. Electrostat., Vol. 69, pp. 296 - 301, 2011.

[6] B. Tabti, R. Mekideche, M. Plopeanu, L.M. Dumitran, L. Herous, L. Dascalescu, Corona charging and charge decay characteristics of nonwoven filter media, IEEE Trans. Ind. Appl., Vol. 46, pp. 634-640. 2010.

[7] B. Tabti, L. Dascalescu, C.M. Plopeanu, A. Antoniu, and R. Mekideche, Factors that influence the corona charging of fibrous dielectric materials. J. Electrostat., vol. 69, pp.193-197, 2009.

[8] A. Samuila, M. Blajan, R. Beleca, M. Huzau, R. Morar, L. Dascalescu, and A. Iuga, ―Modeling of wire corona electrode operation in electrostatic separation at small and large gaps. J. Electrostat., Vol. 63, pp.955-960, 2005

[9] L. Dascalescu, A. Iuga, R. Morar, V. Neamtu, A. Samuila, I. Suarasan, Charging of particulates in the corona field of roll-type electroseparators, J. Phys. D 27, 1242–1251, 1994.

[10] L. Dascalescu, A. Iuga, R. Morar, V. Neamtu, I. Suarasan, A. Samuila, D. Rafiroiu, Corona and electrostatic electrodes for high-tension separators, J. Electrostatics 29, pp. 211–225, 1993.

[11] L. Dumitran, L. Badicu, M. Plopeanu, L. Dăscălescu, Efficiency of Dual Wire-Cylinder Electrodes Used in Electrostatic Separators, Rev. Roum. Sci. Techn., Électrotechn. et Énerg., 55, 2, pp.171 – 180, 2010.

[12] L.M. Dumitran, P. Atten, P.V. Notingher and L. Dascalescu, 2-D corona field computation in configurations with ionising and non-ionising electrodes, J. Electrostatics, 64, pp. 176 – 186, 2005.

[13] 7. L.M. Dumitran, L. Dascalescu, P.V. Notingher, P. Atten, Modeling of corona discharge in cylinder-wire-plate electrode configuration, Journal of Electrostatics, 65, pp. 758 – 763, 2007.

[14] K.R. Parker, Electrostatic Precipitation, Chapman & Hall, New York, 1997.

[15] K. Adamiak, Adaptive approach to finite element modeling of corona fields, IEEE Trans. Ind. Appl. 30, pp. 387–393, 1994.

[16] M. Abdel-Salam, Z. Al-Hamouz, Analysis of monopolar ionized fields as influenced by ion diffusion, IEEE Trans. Ind. Appl. 31, pp. 484–493, 1995.

[17] V. Jaiswal, M.J. Thomas, Finite element modelling of ionized field quantities around a monopolar HVDC transmission lines, J. Phys. D 36, pp.3089–3094, 2003.

[18] J. Davis, J. Hoburg, Wire-duct precipitator field and charge computation using finite element and characteristics methods, J. Electrostat. 14, pp.187–199, 1983.

[19] A.A. Elmoursi, G.S.P. Castle, Modelling of corona characteristics in a .-duct precipitator using the charge simulation technique, IEEE Trans. Ind. Appl. 23, pp. 95–102, 1987.

[20] M. Abouelsaad, M. Abouelatta, A. Salama, Genetic algorithm-optimised charge simulation method for electric field modelling of plate-type electrostatic separators, IET Science, Measurement and Technology, Vol.7,1, pp. 1–7, 2012.

[21] R.S. Sigmond, The unipolar corona space charge flow problem, J. Electrostat. 18, pp.249–272, 1986.

[22] Peek, F. Ionization Phenomena in High Voltage Engineering, (McGraw-Hill, New York, 1929)

[23] Singer, H., Steinbigler, H., Weiss, P.: 'A charge simulation method for the calculation of high voltage fields', IEEE trans., PAS, 1974, 93, pp1660-68, 1974

[24] Rafiroiu, D., Suarasan, I., Morar, R., Atten, P., Dascalescu, L.: 'Corona inception in typical electrode configurations for electrostatic processes applications', IEEE Trans. Ind. Appl. 37, pp.766–771, 2001.

[25] Rafiroiu, D., Morar, R., Atten, P., Dascalescu, L.: 'Premises for the mathematical modeling of the combined corona–electrostatic field of roll-type separators', IEEE Trans. Ind. Appl. 36, pp1260–1266, 2000.

[26] M Abdel-Salam, A Hashem, A Turky and A Abdel Aziz 2007 Corona performance of conductor-to-plane gaps as influenced by underneath grounded and negatively stressed metallic grids J. Phys. D: Appl. Phys. vol. 40, no. 6, pp. 1684–93

[27] T N Tran, I O Golosnoy, P L Lewin and G E Georghiou 2011Numerical modelling of negative discharges in air with experimental validation J. Phys. D: Appl. Phys. vol. 44, no. 1, pp. 5203 .

[28] P Sattari,C F Gallo, G S P Castle and K Adamiak 2011 Trichel pulse characteristics—negative corona discharge in air J. Phys. D: Appl. Phys. vol. 44, no. 15, pp. 5502.

[29] J Q Feng 1999 Application of Galerkin finite-element method with Newton iterations in computing steady-state solutions of unipolar charge currents in corona devices J. Comput. Phys. vol.151, no. 2, pp. 969–989.

[30] K Yanallah, F Pontiga, A Fernandez-Rueda and A Castellanos 2009 Experimental investigation and numerical modeling of positive corona discharge: ozone generation J. Phys. D:Appl. Phys. vol. 42, no. 6, pp. 5202.